Zbl. Vet. Med. B, 24, 367—385 (1977)
© 1977 Verlag Paul Parey, Berlin und Hamburg
ISSN 0514—7166/ASTM-Coden: ZVRBA2

From the Department of Microbiology,
College of Veterinary Medicine and Biomedical Sciences,
Colorado State University, Fort Collins, Colorado, USA
and the Department of Pathology, Arab Development Institute,
Tripoli, Libya

Light and Ultrastructural Pathologic Changes in Intestinal Coronavirus Infection of Newborn Calves*

By

A. M. Doughri and J. Storz

With 14 figures

(Received for publication June 16, 1976)

Introduction

Enteric diseases of newborn animals represent a serious economic problem and may be caused by several different etiologic agents (24). The importance of viruses as causes of enteritis in the newborn became recently evident (8, 9, 11, 14, 15, 16, 21, 25).

The viral cause of transmissible gastroenteritis of newborn pigs (7) was first identified as a coronavirus by Tajima (26). Later coronaviruses were recognized as a cause of enteritis and hepatitis in mice (22), and enteritis of calves (23) and dogs (1).

The coronavirus strain LY-138 used in the present studies had been recovered in 1965 from intestinal samples of newborn diarrheic calves. Several attempts to cultivate this strain in different types of cultured bovine fetal cells were unsuccessful. This viral agent was maintained by oral inoculation and intestinal infection of newborn calves (6).

The purpose of the present study was to describe histopathologic intestinal changes and to relate them to ultrastructural cytopathic features observed in intestinal epithelial cells of newborn calves inoculated orally with LY-138 coronavirus.

Material and Methods

Seven conventional newborn calves were used as principals. They were separated from their dams immediately after birth without access to colostrum.

* These investigations were supported by NIH Research grant AI-08420, Regional Research Funds of Projects W-88 and W-120 and by funds from Jensen-Salsbery Laboratories, Kansas City, Missouri. This paper is published as scientific paper No. 2177, Colorado Agricultural Experiment Station.

They were kept in isolation stalls and were inoculated orally during the first 24 h after birth with a homogenate of intestinal mucosal scrapings containing coronavirus strain LY-138.

The initial inoculum was prepared from intestinal mucosal scrapings of a naturally-infected diarrheic calf (LY-138). Intestinal samples of the experimentally inoculated calves served as viral source to prepare the inoculum for the 7 calves of the present study. Intestinal mucosal scrapings were homogenized in Dulbecco's phosphate buffer solution to make a 10 % homogenate. The homogenate was centrifuged at 3000 xg for 15 min. to eliminate coarse debris. The supernatant fluid was carefully recovered and centrifuged twice at 17,300 xg for 30 min. each in a refrigerated centrifuge. Seventy ml. of the second supernatant was further diluted with Dulbecco's phosphate buffer to make a 200—300 ml. inoculum for each calf. The calves drank the inocula from nippled bottles.

Necropsy examination was performed when the calves reached a moribund stage 30—48 h after inoculation. They were killed by electrocution. The abdominal viscera were exposed at once. Intestinal tissue specimens from the various levels of the intestinal tract were collected. For light microscopic studies tissue specimens were fixed in 10 % neutral buffered formalin. They were processed routinely for paraffin embedding and sectioned at a thickness of 5 μ. Mounted sections were stained with hematoxylin and eosin. Villus-to-crypt ratios were measured in histological sections using an ocular micrometer.

Fig. 1. Villi (v) of the middle jejunum are broader and shorter than normal. Petechial hemorrhages (arrows) are at the tips of denuded villi. Basal lamina (BL) separates the lamina propria from the gut lumen, and remaining epithelial cell lining (ECL) is cuboidal and squamous. Crypts of Lieberkühn (CL) are hypertrophic. H and E stain. 700 ×

For ultrastructural studies, several intestinal 2-mm-wide rings were taken from the different levels of the intestinal tract and placed immediately into a petri dish containing ice-cold 6.25 % phosphate buffered glutaraldehyde at pH 7.2. When the tissue specimens became rigid after 4—5 min., they were cut into 1-mm^3 tissue blocks parallel to the longitudinal axis of the villi and prefixed for 2 h. The specimens were then washed in phosphate-buffered saline solution and postfixed for 1 h in 1 % osmium tetroxide of MILLONIG (18). The tissue blocks were dehydrated and embedded in Epon 812 as described by LUFT (13). They were oriented in flat rubber molds to obtain sections parallel to the longitudinal axis of the microvilli. Ultrathin sections were cut with the MT 2-B ultratome, and they were stained with uranyl acetate (28), followed by lead citrate (20). All specimens were examined with an HU-12 Hitachi electron microscope.

Results

Clinical signs: The calves developed a profuse yellow watery diarrhea 24—30 h after inoculation. There was a slight rise in body temperature with a gradual decline as the calves became moribund. The calves became dehydrated, but they continued to drink milk provided. They reached a moribund stage 30—48 h after oral inoculation. Details of the pathophysiology in newborn calves inoculated with strain LY-138 were reported (19).

Gross pathologic changes: On postmortem examination, abundant foamy yellow fluid was present in the small and large intestines. The small intestinal

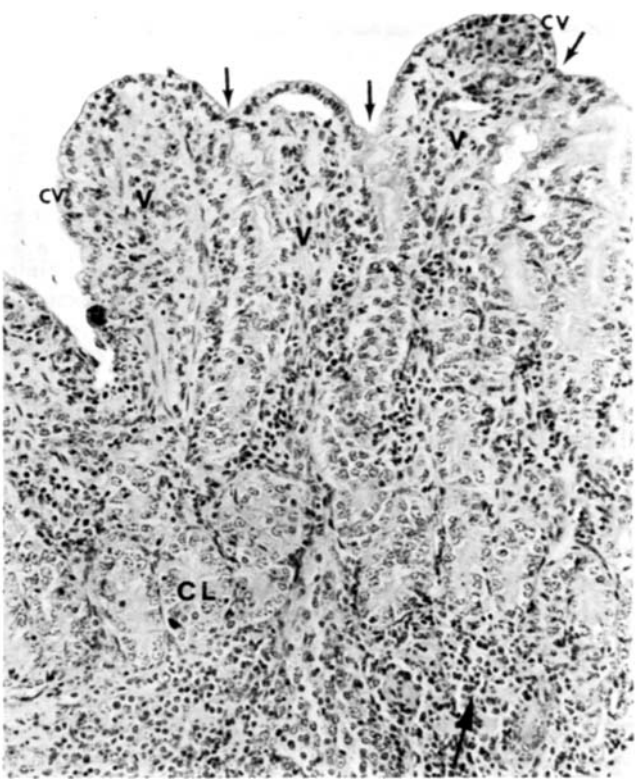

Fig. 2. Villi (v) of proximal jejunum are fused (small arrows) between tips and intervillous zones. Epithelial cell lining is vacuolated (CV). The lamina propria is infiltrated with mononuclear cells (large arrow). CL = crypt of Lieberkühn. H and E stain. 560 ×

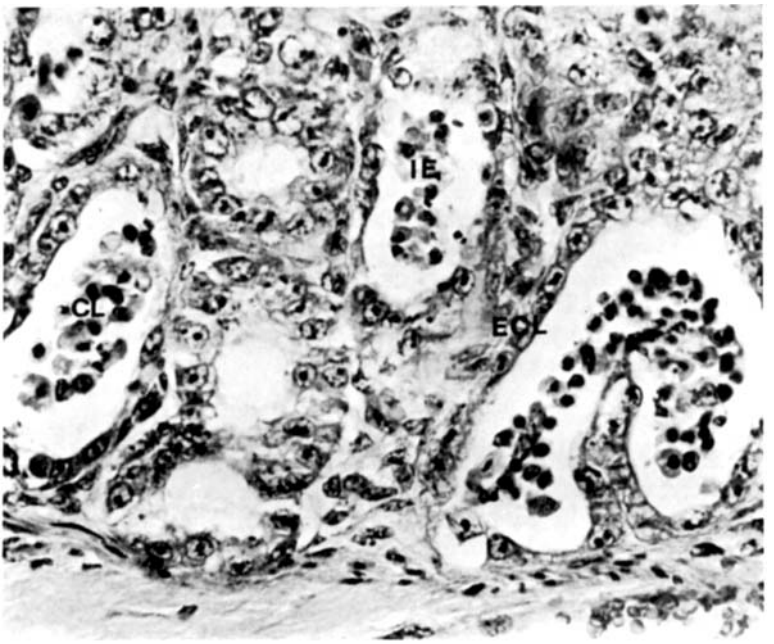

Fig. 3. Crypts of Lieberkühn (CL) are lined with squamous epithelium (ECL). The lumina are dilated with inflammatory exudate (IE), consisting of mononuclear, sloughed epithelial, and a few polymorphonuclear cells. H and E stain. 1,400 ×

wall was atonic and appeared thin and almost transparent in the region of the proximal and middle jejunum. With the exception of the duodenum the intestinal mucosa was hyperemic and had otherwise minimal gross lesions. The stomach was usually filled with milk curds, and the abomasal leaflets were hyperemic and edematous. The mesenteric lymph nodes were enlarged and their associated blood vessels were congested.

Histologic changes: Coronavirus strain LY-138 infected cells of both the small and large intestine of newborn calves. The small intestine, particularly the proximal jejunum, was the site of the most severe histopathologic lesions, and the large intestine was affected to a lesser degree.

The intestinal mucosa of the duodenum appeared normal. The jejunum and ileum had histologic alterations of the mucosal architecture. The villi were shortened and broader than normal with extensive fusion of adjacent villi (Figs. 1, 2). Villus-to-crypt ratios averaged 2 : 1 as compared with a value of 6 : 1 in normal calves. Some villi were denuded above the intervillous zones and had petechial hemorrhages on the apical surface (Fig. 1). Other villi were covered with cuboidal or flattened epithelial cells (Figs. 1, 2). The absorptive epithelial cells had lost their nuclear palisading, and they had vesiculated nuclei and an increased number of vacuoles. Some of these vacuoles were large and contained eosinophilic debris. Other absorptive epithelial cells were at different stages of degeneration and necrosis. Goblet cells were reduced in number. The crypt epithelium became hyperplastic and had an increased number of mitotic figures (Fig. 1). Some crypts of Lieberkühn were distended and contained inflammatory exudate and cellular debris, and had flattened epithelial cell lining (Fig. 3). The lamina propria mucosae was edematous and moderately infiltrated with mononuclear and a few polymorphonuclear cells (Figs. 1, 2). Connective tissue cells were swollen and had proliferated in the

edematous lamina propria mucosae. Blood vessels were dilated and engorged with red blood cells. A few small, superficial focal hemorrhages were observed in the abomasal and intestinal mucosa. Peritonitis characterized by mononuclear cell infiltration was observed in one calf.

The histologic changes in the large intestine were less severe than those of the small intestine. Vacuolation, desquamation, and sloughing of intestinal epithelial cells were evident. The crypts of Lieberkühn were hyperplastic. Some were dilated and their epithelial cell lining had sloughed and degenerated (Fig. 4).

Ultrastructural pathologic changes: Examination of ultrathin sections of the coronavirus-infected intestinal mucosa revealed that infection involved both the villous epithelial cell lining and some cellular components of the lamina propria mucosae. Morphologically, viral replication occurred entirely in the cytoplasm of infected cells with no apparent nuclear involvement. Viral structures were observed enmeshed in electron-dense, granulo-fibrillar material within membrane-bound, cytoplasmic structures and dilated cisternae of the rough endoplasmic reticulum, or within cytoplasmic vacuoles and Golgi vesicles (Figs. 5, 6). In the latter cytoplasmic structures, some but not all virions had fine thread- like projections. Enveloped virions measured approximately 90 nm in diameter (Fig. 5).

Ultrastructural pathologic changes induced by coronavirus infection were not difficult to assess in ultrathin sections. The intestinal villi were lined with low columnar, cuboidal or squamous epithelial cells. Some intestinal villi

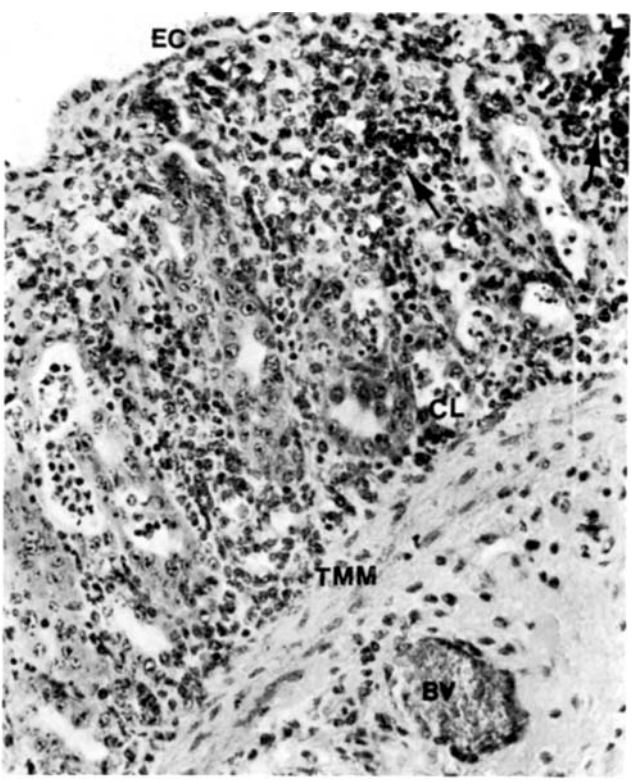

Fig. 4. Notice the cuboidal epithelial cell (EC), the mononuclear cell infiltration (arrows), and affected crypts of Lieberkühn (CL) in section of large intestine. Tunica muscularis mucosae (TMM). Dilated blood vessel engorged with red blood cells. H and E stain. 560 ×

were completely denuded and had no epithelial cell lining (Fig. 7). The lamina propria mucosae of such villi was separated from the gut lumen by a festooned, fragmented basal lamina, and had attached to its epithelial side a few cellular components and viral particles (Fig. 7).

Infected cells were present among apparently normal neighbouring cells. Viral replication occurred mainly in the mature, differentiated absorptive epithelial cells and goblet cells of the villi (Figs. 5, 6, 8). Undifferentiated epithelial cells at the base of the villi as well as fibroblasts and endothelial cells of small blood capillaries of the lamina propria mucosae were occasionally infected (Fig. 9).

The infected absorptive intestinal epithelial cells were at various stages of degeneration and necrosis, depending on the progress of viral development. Cells at the early stage of infection had an increased number of free ribosomes. Large aggregates of single ribosomes were infrequently observed around the

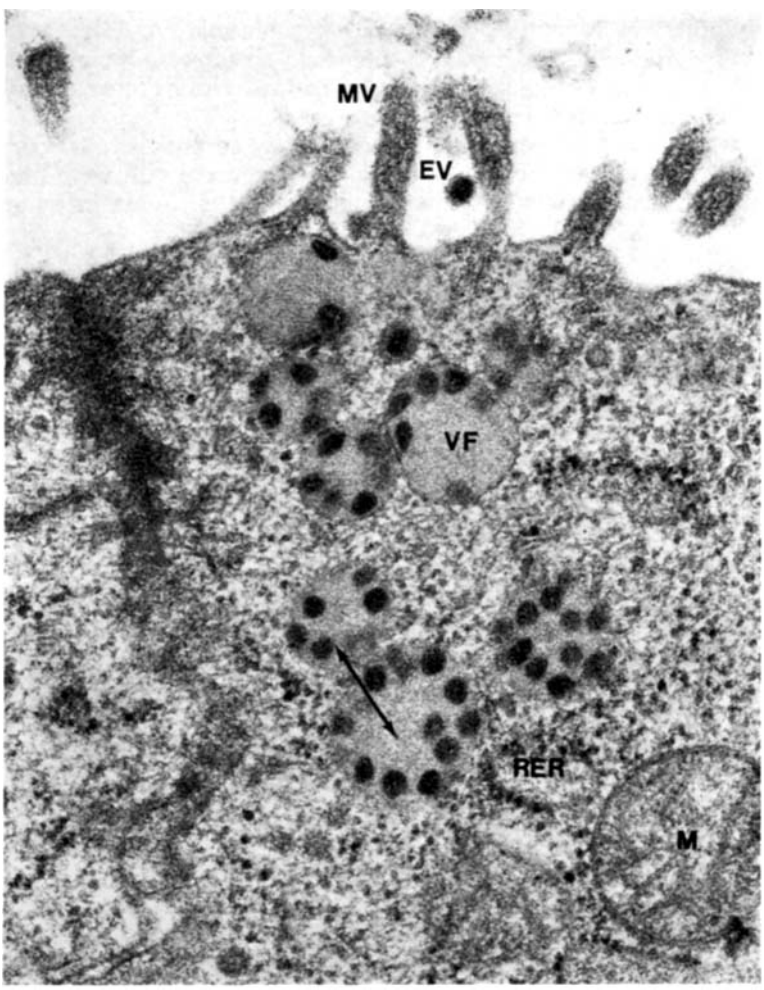

Fig. 5. Absorptive intestinal epithelial cell containing viral factories (VF) some of which are in process of fusion (double-headed arrow), and a few microvilli (MV). Rough endoplasmic reticulum (RER), mitochondrion (M), and enveloped virion (EV). Uranyl acetate-lead citrate stain. 55,000 ×

rough endoplasmic reticulum. Viral structures were not seen to be associated with such aggregates. Distension of smooth and rough endoplasmic reticulum with electron-dense, granulo-fibrillar material was frequently observed (Fig. 10). The rest of the cellular organelles appeared morphologically normal at the early stage of infection of cells. As viral replication progressed, well defined, membrane-bound, round cytoplasmic structures, measuring 0.2 to 0.5 μ. in diameter and filled with granulo-fibrillar, electron-dense material, appeared in the apical cytoplasm of infected cells (Fig. 5). These cytoplasmic structures were considered as viral factories. Embedded in their matrices were varying numbers of viral core structures. Electron-dense, closely packed, convoluted tubular structures were occasionally observed in the cytoplasm of infected cells. The Golgi complex became vesiculated. Large numbers of Golgi vesicles containing viral structures were observed (Figs. 6, 8). At this stage of coronaviral infection, cellular organelles became degenerated, as evidenced

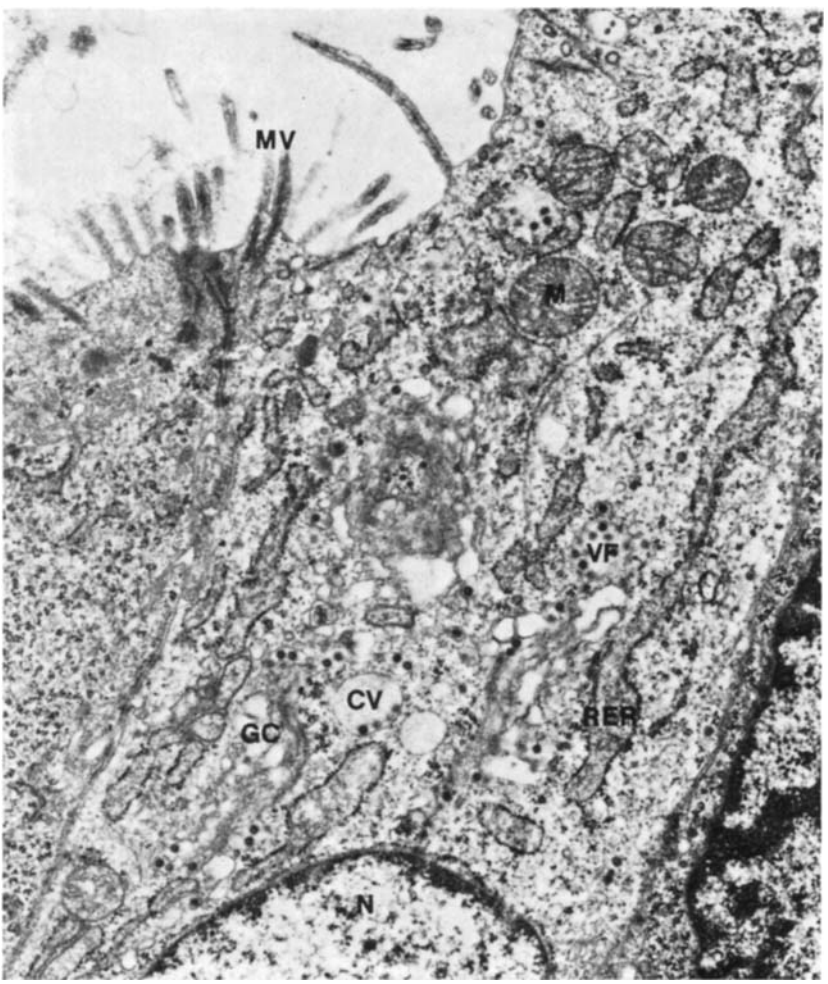

Fig. 6. Infected intestinal absorptive epithelial cell with Golgi complex (GC) vesiculation, virions in Golgi vesicles, dilated rough endoplasmic reticulum (RER), cytoplasmic vacuoles (CV) lined internally with viral particles, and a few distorted microvilli (MV). Mitochondria (M), viral factories (VF). Uranyl acetate-lead citrate stain. 15,200 ×

by fine vacuolation of the cytoplasmic matrix. Mitochondria became swollen and dilated and their number decreased. The space between the nuclear envelopes became wider, but other morphologic changes were not observed in the nucleus.

With the emergence of enveloped virions and release of viral particles, severe degenerative and early necrotic changes affected the cellular organelles. From this stage on, ribosome depletion, loss of electron-density of the cytoplasmic matrix, fragmentation and distortion of mitochondrial cristae, and heterochromatin margination of the nuclei were detected. The cytoplasmic matrix of infected cells was replaced by large numbers of smooth-surfaced, cytoplasmic vacuoles lined internally with viral structures. Large inclusions

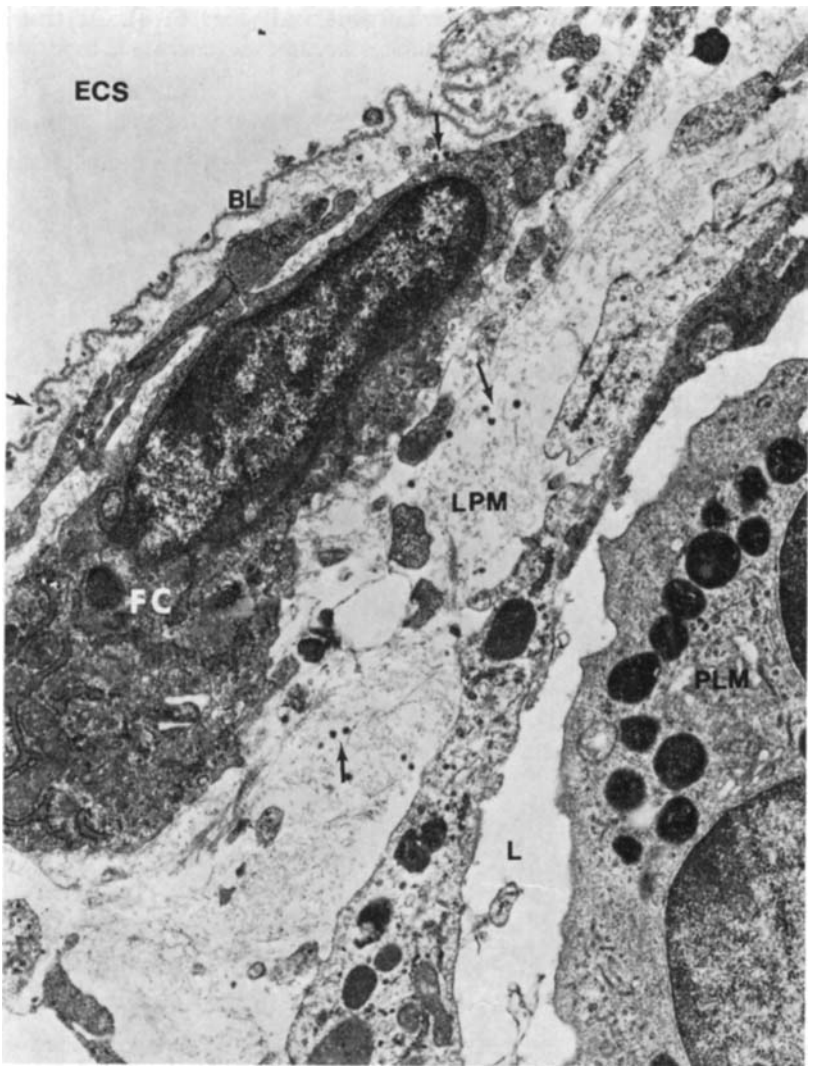

Fig. 7. Denuded epithelial cell surface (ECS) of a villus. Basal lamina (BL) is festooned, fragmented and separates the lamina propria mucosae (LPM) from the gut lumen. Virions (arrows) are present at the epithelial cell surface, surface of a fibroblast (FC) and in the lamina propria mucosa (LPM). Polymorphonuclear (PLM) cell within the lumen (L) of lymphatic channel. Uranyl acetate-lead citrate stain. 12,800 ×

replaced most of the cytoplasmic matrix in some epithelial cells. These inclusions contained numerous viral particles or viral factories, degenerated and necrotic mitochondria, fat droplets, myelin figures and accumulations of lysosome-like material (Fig. 11). The plasmalemma became fragmented and the nuclei became pyknotic and lysed. The microvilli of infected cells had a broad spectrum of pathologic changes. They were normal or slightly altered in the early stages of infection. They were short, distorted, sparse or completely absent over large areas of the epithelium during the late stages of infection (Figs. 5, 6, 9).

The lamina propria mucosae was edematous and infiltrated with a large number of mononuclear cells. The connective tissue cells were swollen, and some fibroblasts were infected. Free virions were seen in the lamina propria mucosae. The endothelial cells of the small blood capillaries were also found to be infected. Free viral particles were seen in the lumina of capillaries (Fig. 12).

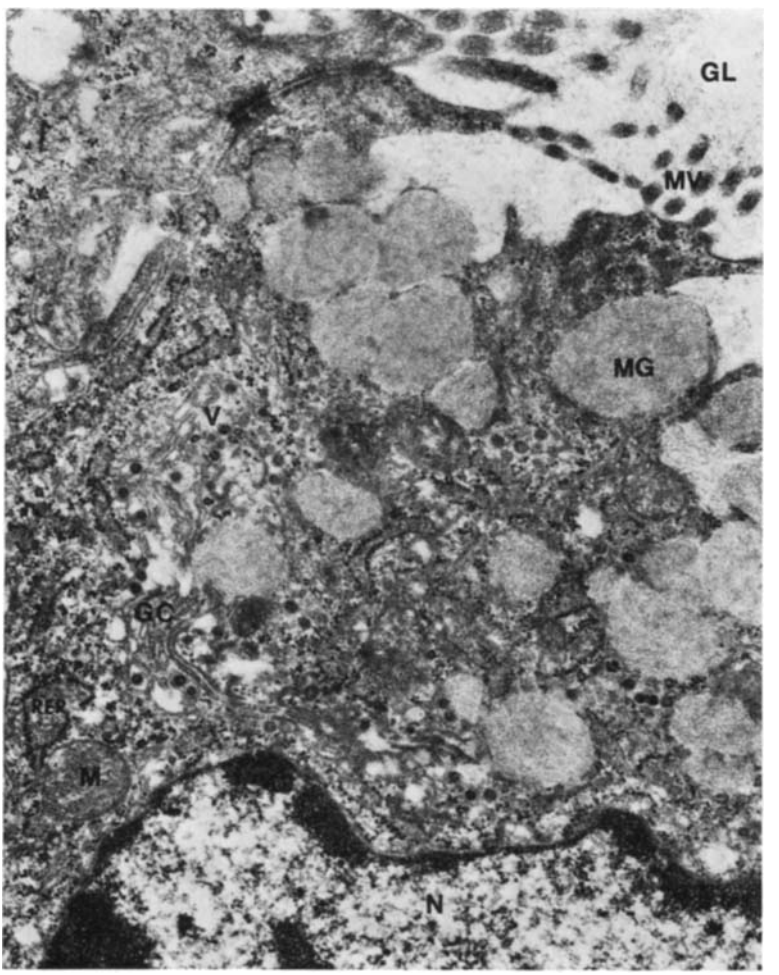

Fig. 8. Golgi complex (GC) of infected goblet cell is vesiculated and contains virions (v) in its vesicles. Mitochondria (M), mucus granules (MG), dilated rough endoplasmic reticulum (RER), microvilli (MV) and gut lumen (GL). Uranyl acetate-lead citrate stain. 20,400 ×

Large numbers of extracellular viral particles were observed free in the gut lumen. Virions often lined the apical plasmalemma and microvilli of normal appearing and infected intestinal epithelial cells (Figs. 9, 13). Virions were also present within the intercellular space of adjacent intestinal epithelial cells (Fig. 14). Desquamated infected epithelial cells were in the gut lumen.

Discussion

Intestinal coronavirus infections leading to diarrhea were studied histologically in pigs, calves and dogs (8, 10, 16, 27). The intestinal changes induced by infection with coronaviruses in piglets and calves were also analyzed by scanning electron-microscopy (17, 29).

This intestinal viral infection has not been studied in depth by transmission electron-microscopy. Light microscopic histologic changes in the intestine of newborn calves were compared with and related to detailed ultrastructural analysis of associated cellular changes. The specimens were from

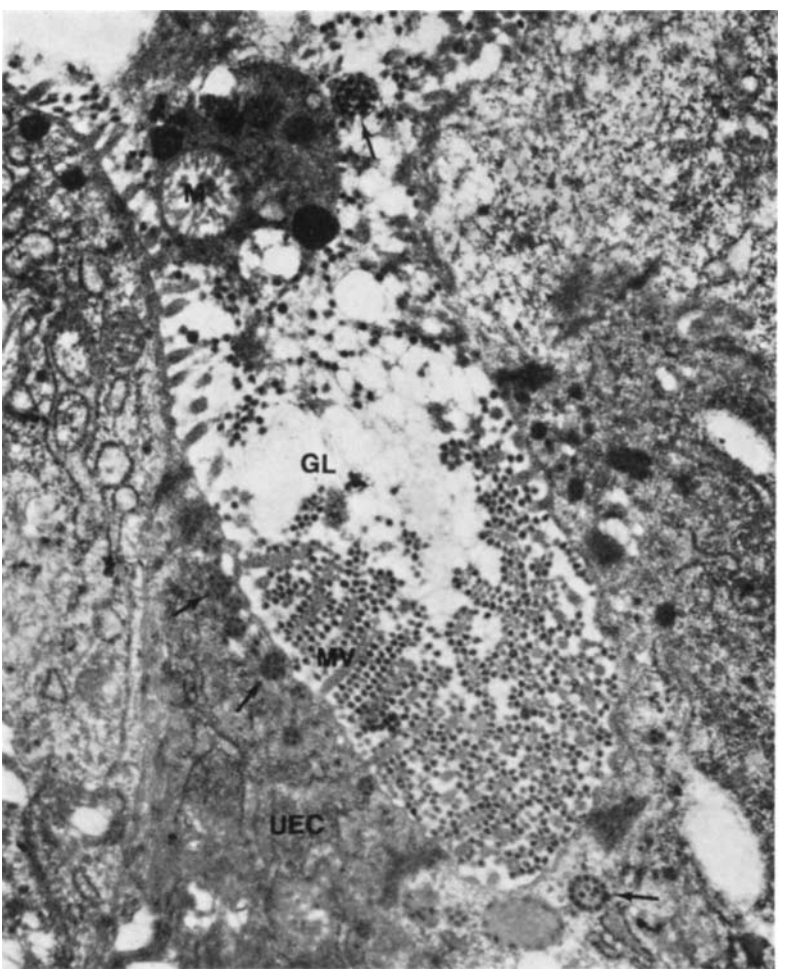

Fig. 9. Virions adsorbed to microvilli (MV) of an infected undifferentiated epithelial cell (UEC) at a base of a villus. Arrow points to viral factories. Gut lumen (GL), degenerated mitochondrion (M) of remnant of an extruded infected epithelial cell. Uranyl acetate-lead citrate stain. 16,800 ×

calves orally inoculated with viral strain LY-138 which has not yet been successfully adapted and propagated in cultured cells and which has morphologic properties of coronaviruses (6).

The histologic changes observed in our investigations were similar to those described by MEBUS and coworkers (16) in calves, and they also corresponded to the basic pattern of changes described in transmissible gastroenteritis of pigs (8, 27) and those induced by coronaviral strain N-71 in dogs (10). After oral ingestion, the coronaviral strain LY-138 infected the absorptive epithelial cell lining of the intestinal villi resulting in atrophy of the villi, decrease in height and extensive sloughing of intestinal epithelial cells that resulted in some denuding. The basis of this change is obviously the excessive rate of cell death from the cytocidal action of the coronavirus.

The clubbing of the intestinal villi probably resulted from the dilation of the small blood capillaries at the apices of the villi, from edema and increased cellularity of the lamina propria mucosa of the villi. The extensive fusion of villi can be attributed to the fact that swollen and shorter villi are less mobile and tend to adhere to each other.

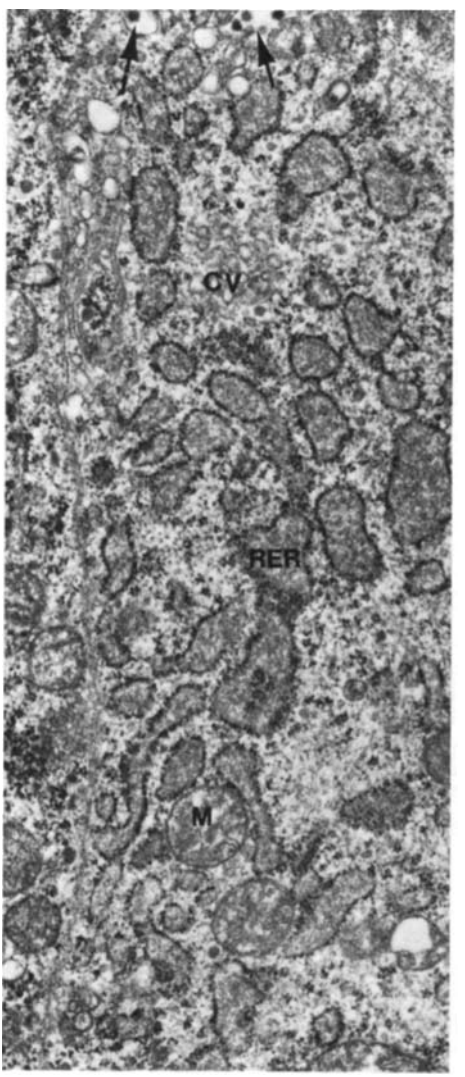

Fig. 10. Extensive dilation of the rough endoplasmic reticulum network (RER) of an infected absorptive intestinal epithelial cell. A few virions (arrows) are present within Golgi vesicles. Mitochondria (M), early cytoplasmic vesiculation (CV). Uranyl acetate-lead citrate stain. 16,000 ×

The absorptive intestinal epithelial cells became vacuolated. Some of the large vacuoles contained eosinophilic debris. These cytoplasmic inclusion-like

structures can be detected in the light microscope. They contained, as revealed ultrastructurally, viral particles, viral factories and lysosome-like structures and were usually bounded by a membrane.

While scanning electron microscopy gave valuable information of the topography of the lesion in an organ like the intestinal tract, transmission electron microscopy granted us insight into the affected cells. The range of infected cells could be clearly identified. The different stages of viral morphogenesis were correlated to changes in cellular organelles and to the gradual progress of the cytocidal action. Observations on the behavior of cellular organelles in the course of viral multiplication gave an indication of the loss of cellular functions, which may contribute to the pathogenesis of an intestinal disease before the ultimate death of infected cells.

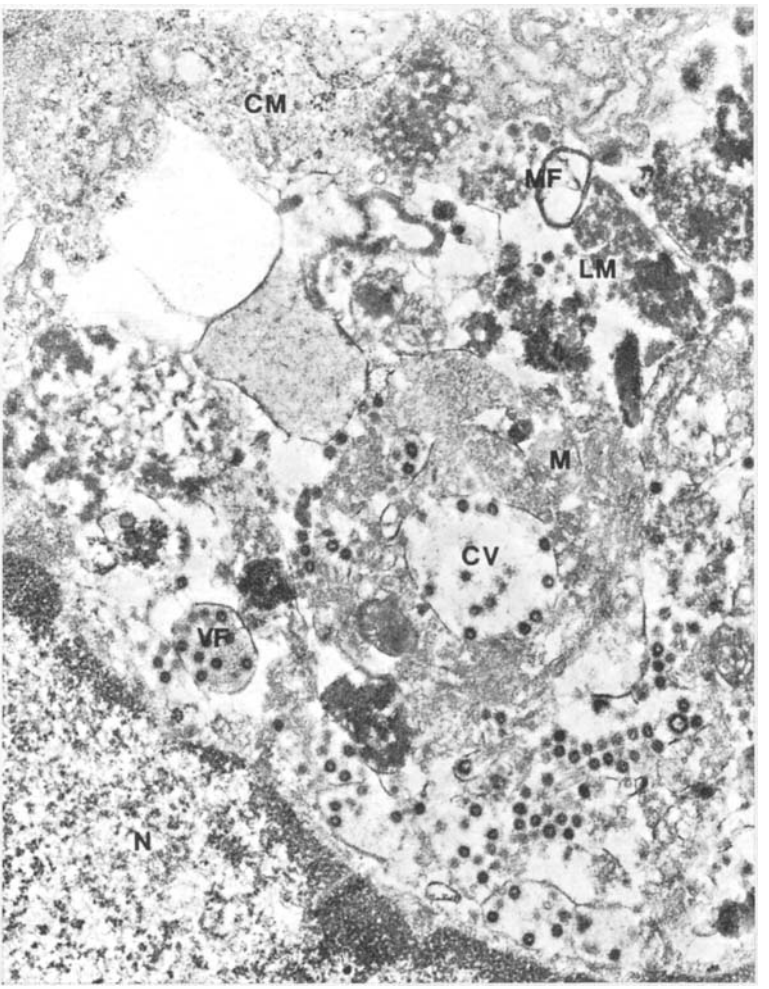

Fig. 11. Apical cytoplasmic matrix (CM) of an infected intestinal absorptive epithelial cell replaced by a large inclusion consisting of viral factories (VF), virions, cytoplasmic vacuoles (CV) lined internally with virions, lysosome-like material (LM), myelin figures (MF), and a cluster of mitochondria (M). Nucleus (N). Uranyl acetate-lead citrate stain. 24,000 ×

The virions of coronaviral strain LY-138 interacted with the glycocalyx and adsorbed to microvilli and were taken up through the brush border of the absorptive intestinal epithelial cells. They also were seen in the intercellular spaces of neighbouring intestinal epithelial cells and appeared to enter cells through the lateral cell membrane by fusion. The mechanisms by which this coronaviral strain penetrates the glycocalyx and by which it gains access into intercellular spaces should be explored further.

The absorptive intestinal epithelial cell was the cell type most frequently infected, but the virus also replicated in goblet cells and undifferentiated epithelial cells of the villi, and in fibroblasts and endothelial cells of small blood capillaries of the lamina propria mucusae.

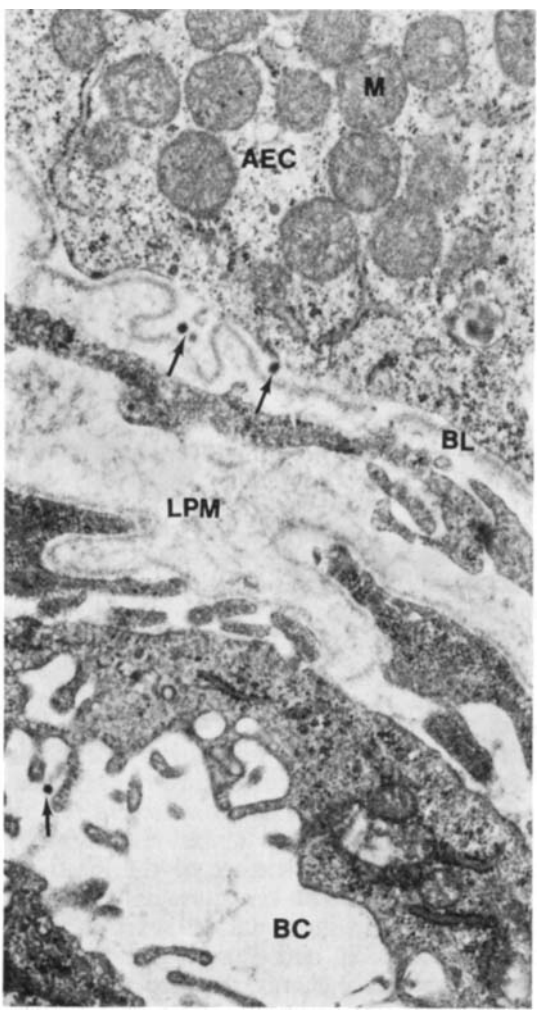

Fig. 12. Virions (arrows) at the basal portion of absorptive epithelial cell (AEC) and in the lumen of small blood capillary (BC). Basal lamina (BL) is festooned and fragmented. Mitochondria (M), lamina propria mucosae (LPM). Uranyl acetate-lead citrate stain. 16,000 ×

There was an interesting pattern of involvement and reaction of cellular organelles in this coronaviral infection. The rough and smooth endoplasmic reticulum became dilated and filled with electron-dense, granulo-fibrillar material. Membrane-bound viral factories occupied large areas of the supranuclear cytoplasm of infected absorptive intestinal epithelial cells. Viral cores condensed in the electron-dense, granulo-fibrillar material within viral factories and the rough endoplasmic reticulum. The possible significance of this reaction in coronaviral morphogenesis was described elsewhere (6). Cytoplasmic vacuoles and Golgi vesicles formed during the process of virus matura-

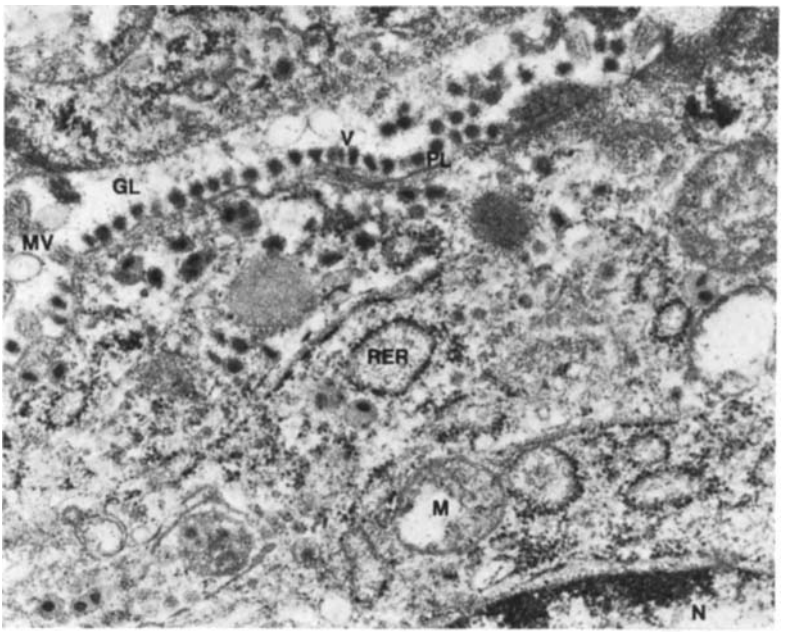

Fig. 13. Virions (v) lining the apical plasmalemma (PL) of an infected absorptive epithelial cell. Notice the scarcity of microvilli (MV). Mitochondrion (M), gut lumen (GL), nucleus (N). Uranyl acetate-lead citrate stain. 28,000 ×

tion rather than with secondary degeneration after virus production. The increased formation of cytoplasmic vacuoles, the vesiculation of the Golgi complex, and the decrease in cellular ribosomes are directly induced by some process necessary for viral multiplication and maturation. The mitochondria became swollen and dilated and their number decreased. The microvilli became shorter, distorted and sparse, and pinocytotic vesicles were absent in cells at intermediate and later stages of infection.

The profuse diarrhea that the calves developed after oral inoculation may be explained by the loss of function of infected cells during viral replication and the subsequent cytocidal action which leads to an excessive rate of cell death. The microvillous border became excessively damaged and normally functions as an important digestive and adsorptive surface of the intestinal cell (3). The pinocytotic system, the rough and smooth reticulum network, and the Golgi elements have significant functions in intestinal cell transport and biosynthesis. The relatively rapid degeneration and loss of mitochondria impaired the ability of intestinal cells to generate energy required specifically for active transport functions in absorptive intestinal epithelial cells. All these changes in cellular organelles are likely to contribute to intestinal dysfunction and malabsorption.

Although the histological changes induced by coronavirus infection were remarkably consistent in all calves and were similar to those described in pigs with transmissible gastroenteritis (8, 27) and dogs with coronavirus enteritis (10), at present none of these changes should be considered as specific or pathognomonic for this infection. The specificity of these changes should be clarified and compared with other intestinal infections with obligate intracellular parasites. Increased desquamation, vacuolation and the related decrease in height of intestinal epithelial cells probably results from any

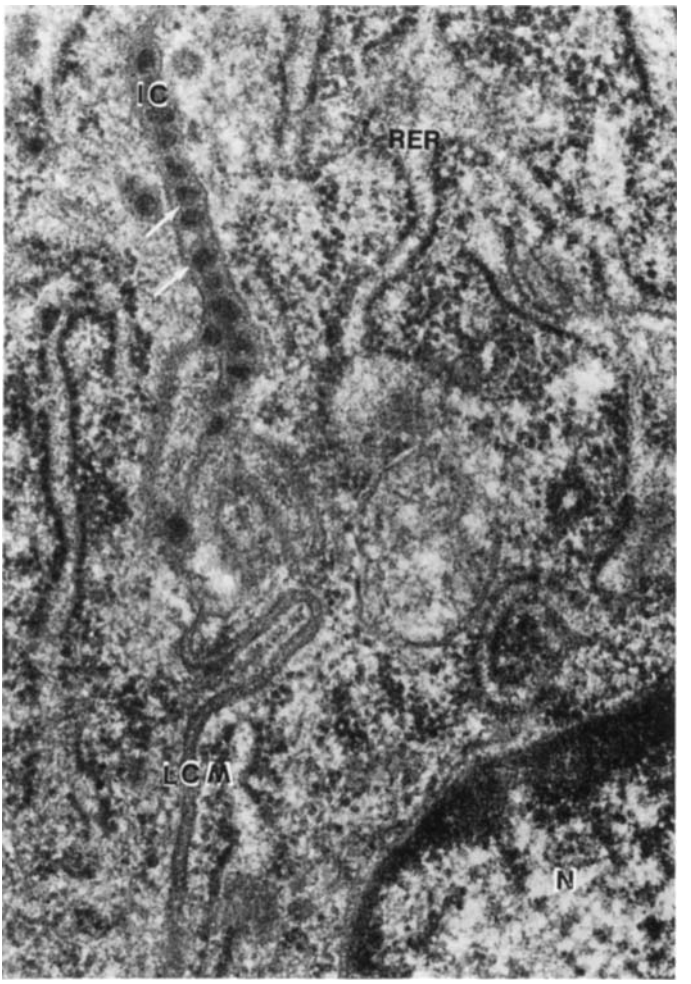

Fig. 14. Virions (arrows) in the intercellular space (IC) of the lateral cell membranes (LCM) of adjacent intestinal absorptive epithelial cells. Nucleus (N), rough endoplasmic reticulum (RER). Uranyl acetate-lead citrate stain. 48,000 ×

cytocidal infection of the absorptive intestinal epithelial cells. This feature was seen in intestinal chlamydial infections of calves (5). Clubbing and fusion of villi, edema, cell infiltration of the lamina propria as well as festooning and fragmentation of the basal lamnia were features also found in the intestinal chlamydial infections of calves. Finally, the hypertrophy and dilation of the crypts of Lieberkühn were observed in intestinal chlamydial (4, 5) and parvoviral infections (2, 12). It becomes more and more evident that intestinal infections with viruses or chlamydial agents should be studied and compared on a cell biological and ultrastructural basis.

Summary

Seven conventional newborn calves were inoculated orally with the coronavirus strain LY-138, originally recovered from naturally-infected diarrheic calves. All calves developed diarrhea during the first 24 h after

inoculation. The presence and excretion of virus was monitored by electron microscopy.

Grossly, the changes were subtle and not striking. The intestinal tract was distended and contained a yellow clear fluid. The small intestinal wall was thin and transparent.

Histologic changes were characterized by atrophy and fusion of the villi, decreased height and vacuolation of the intestinal epithelial cells, by a reduced number of goblet cells, crypt hypertrophy and dilatation, and by edema and increased cellularity of the *lamina propria mucosae.*

Ultrastructurally the viral agent infected the intestinal absorptive epithelial cells, undifferentiated epithelial cells and goblet cells of the villi, and occasionally fibroblasts and endothelial cells of the *lamina propria mucosae.* Morphologic evidence indicated that virus multiplication occurred only in the cytoplasm of infected cells. The rough and smooth endoplasmic reticulum became dilated, and electron-dense, granulo-fibrillar material filled their cysternae to form smooth membrane-bounded viral factories in the supranuclear cytoplasm of infected intestinal epithelial cells. Ultrastructural cytologic changes in this viral infection consisted of dilation of the endoplasmic reticulum network, cellular ribosome depletion, extensive endoplasmic vacuolation and vesiculation of Golgi elements of intestinal epithelial cells, swelling and degeneration of mitochondria, loss of normal nuclear polarity with pyknosis and karyolysis of the nuclei, loss of cytoplasmic matrix, and a broad spectrum of pathologic changes involving the microvilli and terminal web.

Zusammenfassung

Lichtmikroskopische und Ultrastrukturelle pathologische Veränderungen bei intestinaler Coronavirusinfektion neugeborener Kälber

Sieben konventionelle neugeborene Kälber wurden oral mit dem Coronavirus-Stamm LY-138, der ursprünglich von natürlich infizierten Kälbern mit Diarrhoe stammt, infiziert. Alle Kälber entwickelten Durchfall während der ersten 24 Stunden nach Inokulation. Vorhandensein und die Ausscheidung des Virus wurden elektronenoptisch verfolgt.

Sichtbare Veränderungen waren gering und wenig auffallend. Der Darmtrakt war erweitert und enthielt eine gelbe, klare Flüssigkeit. Die Dünndarmwand war dünn und durchscheinend.

Histologische Veränderungen waren charakterisiert durch Atrophie und Verschmelzung der Zotten, verminderte Höhe und Vakuolisierung der intestinalen Epithelzellen, durch eine reduzierte Anzahl von Gobletzellen, Kryptenhypertrophie und -erweiterung, sowie Ödematisierung und erhöhte Zellularität der *lamina propria mucusae.* Ultrastrukturell infizierte das Virus die intestinalen absorptiven Epithelzellen, nichtdifferenzierte Epithelzellen und Gobletzellen der Zotten, und gelegentlich Fibroblasten sowie Endothelzellen der *Lamina propria mucosae.* Die morphologischen Veränderungen weisen darauf hin, daß die Virusvermehrung nur im Zytoplasma infizierter Zellen stattfand. Das rauhe und glatte endoplasmatische Retikulum war erweitert, und elektronendichtes, granulo-fibrilläres Material füllte die Zisternen aus, die feine Membran-gebundene Virusvermehrungsfabriken in dem supranukleären Zytoplasmabereich infizierter intestinaler Epithelzellen bildeten. Ultrastrukturelle zytologische Veränderungen bestanden bei dieser Virusinfektion aus Erweiterung des endoplasmatischen Retikulumnetzwerks, zellulärem Ribosomenverlust, extensiver endoplasmatischer Vakuolisierung der Golgielemente der intestinalen Epithelzellen, Schwellung und Degeneration von Mitochondrien, Verlust der normalen nukleären Polarität mit Pyknose und Karyolyse der Zellkerne,

Verlust der Zytoplasmamatrix, und aus einem breiten Spektrum pathologischer Veränderungen an den Mikrozotten und der terminalen Netzstruktur.

Résumé

Lésions pathologiques ultrastructurelles et au microscope optique lors d'infection intestinale à Coronavirus chez des veaux nouveau-nés

Sept veaux nouveau-nés conventionnels ont été infectés oralement par la souche LY-138 de Coronavirus, isolée précédement chez des veaux naturellement infectés présentant une diarrhée. Tous les veaux développèrent une diarrhée durant les premières 24 heures suivant l'inovulation. La présence et la sécrétion du virus ont été suivies au microscope électronique.

Les lésions apparentes furent faibles et peu apparentes. Le tractus digestif fut élargi et contenait un liquide jaune et clair. La paroi de l'intestin grêle était mince et transparente.

Les lésions histologiques furent caractérisées par une atrophie et une fusion des villi, une hauteur diminuée et une vacuolisation des cellules épithéliales de l'intestin, par un nombre réduit des cellules caliciformes, une hypertrophie et un élargissement des cryptes ainsi qu'un oedème et un nombre de cellules augmenté de *Lamina propria mucosae*.

Le virus a infecté ultrastructurellement les cellules épithéliales absorbantes de l'intestin, des cellules épithéliales non différenciées et des cellules caliciformes des villi, de temps en temps des fibroblastes et des cellules endothéliales de *Lamina propria mucosae*. Les lésions morphologiques ont montré que la multiplication du virus n'avait lieu que dans le cytoplasme des cellules infectées. Le Reticulum endoplasmique grossier et fin fut élargi et un matériel granuleux et fibrillaire remplissait les citernes qui formaient de fines régions de réplication virale liées à la membrane dans le voisinage cytoplasmique supranucléaire des cellules épithéliales infectées de l'intestin. Les lésions cytologiques ultrastructurelles lors de cette infection virale consistèrent en un élargissement du réseau endoplasmique, une perte des ribosomes cellulaires, une vacuolisation endoplasmique extensive des éléments de Golgi dans les cellules épithéliales de l'intestin, une enflure et une dégénérescence des mitochondries, une perte de la polarité nucléaire normale avec une picnose et une carylolyse des noyaux cellulaires, une perte de la matrice cytoplasmique et un large éventail de lésions pathologiques des microvilli et des tissus terminaux.

Resumen

Modificaciones patológicas fotomicroscópicas y ultraestructurales en la infección intestinal de terneros recién nacidos por virus Corona

Se infectaron por vía oral siete terneros convencionales con la estirpe de virus Corona LY-138, la cual es originaria de terneros, infectados naturalmente, con diarrea. Todos los terneros manifestaban diarrea durante las 24 horas primeras después de la inoculación. Se seguía electrónicoópticamente la presencia y eliminación de virus.

Las modificaciones visibles eran escasas y se destacaban poco. El tracto intestinal se hallaba dilatado, conteniendo un líquido amarillo claro. La pared del intestino delgado era tenue y translúcida.

Las modificaciones histopatológicas se caracterizaban por atrofia y soldadura de las villosidades, altura reducida y vacuolización de las células epiteliales intestinales, por una cantidad reducida de células caliciformes, hipertrofia y ensanchamiento de las criptas, y por edematización y celularidad aumentada de la *lámina propia mucosa*. El virus infectaba ultraestructuralmente las células

epiteliales intestinales absortivas, células epiteliales no diferenciadas y células caliciformes de las villosidades, y, en ocasiones fibroblastos y células endoteliales de la *lámina propia mucosa*. Las modificaciones morfológicas señalan que la multiplicación de virus solo tuvo lugar en el citoplasma de las células infectadas. El retículo endoplasmático basto y fino se hallaba dilatado y material granulosofibrilar, opaco a los electrones, ocupaba las cisternas, las cuales formaban lugares finos de replicación antiviral, ligados a las membranas en el ámbito citoplasmático supranuclear de células epiteliales intestinales infectadas. Las modificaciones citológicas ultraestructurales consistían en esta infección a virus en dilatación del retículo endoplasmático, pérdida celular de ribosomas, vacuolización endoplasmática extensiva de los elementos de Golgi de las células epiteliales intestinales, tumefacción y degeneración de mitocondrias, pérdida de la polaridad nuclear normal con picnosis y cariolisis de los núcleos celulares, pérdida de la matriz citoplasmática, y en un espectro amplio de modificaciones patológicas en las microvillosidades y tejidos terminales.

References

1. BINN, L. N., E. C. LAZAR, K. P. KEENAN, D. L. HUXSOLL, R. H. MARCHWIECI and A. J. STRANO, 1975: Recovery and characterization of a coronavirus from military dogs with diarrhea. Proc. 78th Ann. Meeting, U. S. Animal Health Assoc., 359—366.
2. CARLSON, J. H., F. W. SCOTT and J. R. DUNCAN, 1977. Feline panleukopenia I. Pathogenesis in germfree and specific pathogen-free cats. Vet. Path. *14*, 79—88.
3. CRANE, R. K., 1966: Enzymes and malabsorption: A concept of brush border membrane disease. Gastroenterology. *50*, 254—262.
4. DOUGHRI, A. M., K. P. ALTERA, J. STORZ and A. K. EUGSTER, 1973: Ultrastructural changes in the chlamydia-infected ileal mucosa of newborn calves. Vet. Path. *10*, 114—123.
5. DOUGHRI, A. M., S. YOUNG and J. STORZ, 1974: Pathologic changes in intestinal chlamydial infection of newborn calves. Am. J. Vet. Res. *35*, 939—944.
6. DOUGHRI, A. M., J. STORZ, I. HAJER and H. S. FERNANDO, 1976: Morphology and morphogenesis of a coronavirus infecting intestinal epithelial cells of newborn calves. J. Exptl. Mol. Path. (in press).
7. DOYLE, L. P., and L. M. HUTCHINGS, 1946: A transmissible gastroenteritis in pigs. J. Am. Vet. Med. Assoc. *108*, 257—259.
8. HAELTERMAN, E. O., and B. E. HOOPER, 1967: Transmissible gastroenteritis of swine as a model for the study of enteric disease. Gastroenterology. *53*, 109—113.
9. KAPIKIAN, A. Z., H. W. KIM, R. G. WYATT, W. J. RODRIGUEZ, S. ROSS, W. L. CLINE, R. H. PARROTT and R. M. CHAWOCK, 1974: Reovirus-like agent in stools: Association with infantile diarrhea and development of serologic tests. Science. *185*, 1049—1053.
10. KEENAN, K. P., H. R. JERVIS, R. H. MARCHWICKI and L. N. BINN, 1976: Intestinal infection of neonatal dogs with canine coronavirus 1-71: Studies by virologic, histologic, histochemical and immunofluorescent techniques. Am. J. Vet. Res. *37*, 247—256.
11. LAMBERT, G., A. L. FERNELIUS and N. F. CHEVILLE, 1969: Experimental bovine viral diarrhea in neonatal calves. J. Am. Vet. Med. Assoc. *154*, 181—189.
12. LANGHEINRICH, K. A., and S. W. NIELSON, 1971: Histopathology of feline panleukopenia: A report of 65 cases. J. Am. Vet. Med. Assoc. *158*, 863—872.
13. LUFT, J., 1961: Improvements in epoxy resin embedding methods. J. Biophysic. Biochem. Cytol. *9*, 409—414.
14. MATTSON, D. E., 1973: Adenovirus infection in cattle. J. Am. Vet. Med. Assoc. *163*, 894—896.
15. MEBUS, C. A., E. L. STAIR, M. B. RHODES and M. J. TWIEHAUS, 1971: Pathology of neonatal calf diarrhea induced by a reo-like virus. Vet. Path. *8*, 490—505.
16. MEBUS, C. A., E. .L STAIR, M. B. RHODES and M. J. TWIEHAUS, 1973: Pathology of neonatal calf diarrhea induced by a coronavirus-like agent. Vet. Path. *10*, 45—64.
17. MEBUS, C. A., L. E. NEWMAN and E. L. STAIR, 1975: Scanning electron, light, and immunofluorescent microscopy of intestine of gnotobiotic calf infected with calf diarrheal coronavirus. Am. J. Vet. Res. *36*, 1719—1725.
18. MILLONIG, G., 1961: Advantages of a phosphate buffer for OsO_4 solutions in fixation. J. Appl. Phys. *32*, 1637.
19. PHILLIPS, R. W., and L. D. LEWIS, 1973: Viral induced changes in intestinal transport and resultant body fluid alterations in neonatal calves. Ann. Rech. Vétér. *4*, 87—89.

20. Reynolds, E. S., 1963: The use of lead citrate at high pH as an electron-opaque stain in electron microscopy. J. Cell Biol. *17*, 208—213.
21. Romvary, J., 1964: Incidence of virus diarrhea among newborn calves. Acta. Veterinaria. *15*, 341—347.
22. Rowe, W. P., J. W. Hartley and W. I. Capps, 1963: Mouse hepatitis virus infection as a highly contagious, prevalent, enteric infection of mice. Proc. Soc. Exp. Biol. Med. *112*, 161—165.
23. Stair, E. L., M. B. Rhodes, R. G. White and C. A. Mebus, 1972: Neonatal calf diarrhea: Purification and electron microscopy of a coronavirus-like agent. Am. J. Vet. Res. *33*, 1147—1156.
24. Storz, J., J. R. Collier, A. K. Eugster and K. P. Altera, 1971: Intestinal bacterial changes in chlamydia-induced primary enteritis of newborn claves. New York Acad. Sci. *176*, 162—175.
25. Storz, J., and R. C. Bates, 1973: Parvovirus infections in calves. J. Am. Vet. Med. Assoc. *163*, 884—886.
26. Tajima, N., 1970: Morphology of transmissible gastroenteritis virus of pigs: A possible member of coronaviruses. Arch. Ges. Virusforsch. *29*, 105—108.
27. Trapp, A. L., V. L. Sanger and E. Stalnaker, 1966: Lesions of the small intestinal mucosa in transmissible gastroenteritis-infected germfree pigs. Am. J. Vet. Res. *21*, 1695—1702.
28. Watson, M. L., 1958: Staining of tissue sections for electron microscopy with heavy metals. J. Biophysic. Biochem. Cytol. *4*, 475—478.
29. Waxler, G. L., 1972: Lesions of transmissible gastroenteritis in pigs as determined by scanning microscopy. Am. J. Vet. Res. *33*, 1323—1328.

Address of authors: Department of Microbiology, College of Veterinary Medicine and Biomedical Sciences, Colorado State University, Fort Collins, Colorado 80523, USA.